THE JOURNAL OF PHYSICAL CHEMISTRY Letters

Letter

Cite This: J. Phys. Chem. Lett. 2019, 10, 655−660

pubs.acs.org/JPCL

Investigation into the Photoluminescence Red Shift in Cesium Lead Bromide Nanocrystal Superlattices

Dmitry Baranov,*[,†] Stefano Toso,[†] Muhammad Imran,[†,‡] and Liberato Manna*[,†]

[†]Nanochemistry Department, Istituto Italiano di Tecnologia, Via Morego 30, 16163 Genova, Italy

[‡]Dipartimento di Chimica e Chimica Industriale, Università degli Studi di Genova, Via Dodecaneso 31, 16146 Genova, Italy

Supporting Information

ABSTRACT: The formation of cesium lead bromide ($CsPbBr_3$) nanocrystal superlattices (NC SLs) is accompanied by a red shift in the NC photoluminescence (PL). The values of the PL red shift reported in the literature range from none to ∼100 meV without unifying explanation of the differences. Using a combination of confocal PL microcopy and steady-state optical spectroscopies we found that an overall PL red shift of ∼96 meV measured from a macroscopic sample of $CsPbBr_3$ NC SLs has several contributions: ∼ 10−15 meV from a red shift in isolated and clean SLs, ∼ 30 meV from SLs with impurities of bulklike $CsPbBr_3$ crystals on their surface, and up to 50 meV or more of the red shift coming from a photon propagation effect, specifically self-absorption. In addition, a self-assembly technique for growing micron-sized NC SLs on the surface of perfluorodecalin, an inert perfluorinated liquid and an antisolvent for NCs, is described.

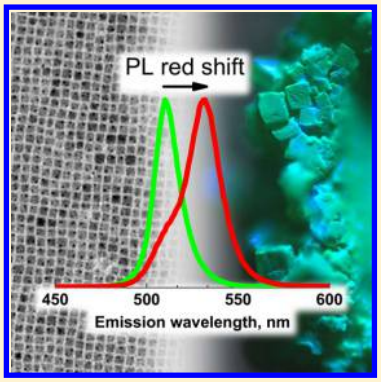

Research into semiconductor cesium lead halide perovskite (LHP) nanocrystals (NCs) has rapidly developed since their hot-injection synthesis was introduced in 2015.[1−3] $CsPbBr_3$ NCs and related materials are currently synthesized with narrow size distributions,[1,4−7] which naturally leads to investigations on their self-assembly capabilities. One motivation to prepare $CsPbBr_3$ NC superlattices (SLs) is to study the coupling between neighboring NCs, resulting in a collective behavior such as exciton delocalization or carrier transport.[8−12] The reports on intriguing optical properties of $CsPbBr_3$ NC SLs such as a tunable anisotropic light emission[13] or superfluorescence[14] indicate that these SLs are promising for applications in light emitting devices.[15] However, the poor compatibility of $CsPbBr_3$ NCs with polar solvents[16] (for example, methanol, 2-propanol, and diethylene glycol) prevents their self-assembly by antisolvent diffusion[17] or at the interface with a polar solvent,[18] singling out slow solvent evaporation as the sole method for preparing SLs. Compared to NC materials that have been studied for a long time, such as CdSe or FePt,[17−19] research on the preparation of SLs from inorganic or mixed LHP NCs is still in its early stages and is in need of new approaches.[15,20]

In this work, we introduce a solvent diffusion technique for growing $CsPbBr_3$ NC SLs on the surface of liquid perfluorodecalin (PFD). PFD, an inert perfluorinated liquid that is partially miscible with hexane, also plays the role of an antisolvent: when a hexane solution of NCs is deposited on top of PFD, hexane gradually diffuses into the PFD, initiating SL nucleation and growth. Using this method, we were able to produce three-dimensional and nearly isotropic SLs with dimensions up to ∼70 μm using quantum-confined $CsPbBr_3$ NCs. An important advantage of growing SLs on top of a liquid over more traditional methods of slow solvent evaporation that are typically bound to a specific substrate is that SLs can be transferred onto silicon or glass substrates.

A second important finding of this work concerns the nature of the photoluminescence (PL) red shift of $CsPbBr_3$ NCs in SLs. $CsPbBr_3$ NCs are bright emitters, and changes in their PL spectra can be indicative of interparticle interactions inside a SL. Specifically, a PL red shift is often an indication of electronic coupling between NCs when they are packed into a solid. Several studies have reported that $CsPbBr_3$ NC SLs exhibit a PL red shift in comparison to NCs in solution, but the extent of this red shift varies from a few millielectronvolts[7,20,21] up to ∼100 meV.[3,15,22,23] Here, we report that individual SLs with a clean surface have a small PL red shift of ∼10−15 meV in comparison to NCs in dilute solution. However, a macroscopic sample of aggregated NC SLs shows a PL red shift of up to ∼96 meV (Figures S1 and S2). Our data indicate that such an increase in the PL red shift arises from at least two additional factors: the presence of SLs covered in impurities with a red-shifted PL (which can add up to ∼30 meV, the impurities being identified as submicrometer particles of $CsPbBr_3$) and a photon propagation effect (which can add another ∼10−50 meV or more due to self-absorption).

The preparation of cube-shaped $CsPbBr_3$ NCs was performed by modifying the method that was developed by Protesescu et al.[1] In short, NCs were synthesized by the hot injection of a cesium oleate precursor into lead bromide that had been dissolved in a mixture of oleic acid, oleylamine, and 1-

Received: January 21, 2019
Accepted: January 24, 2019
Published: January 24, 2019

DOI: 10.1021/acs.jpclett.9b00178
J. Phys. Chem. Lett. 2019, 10, 655−660

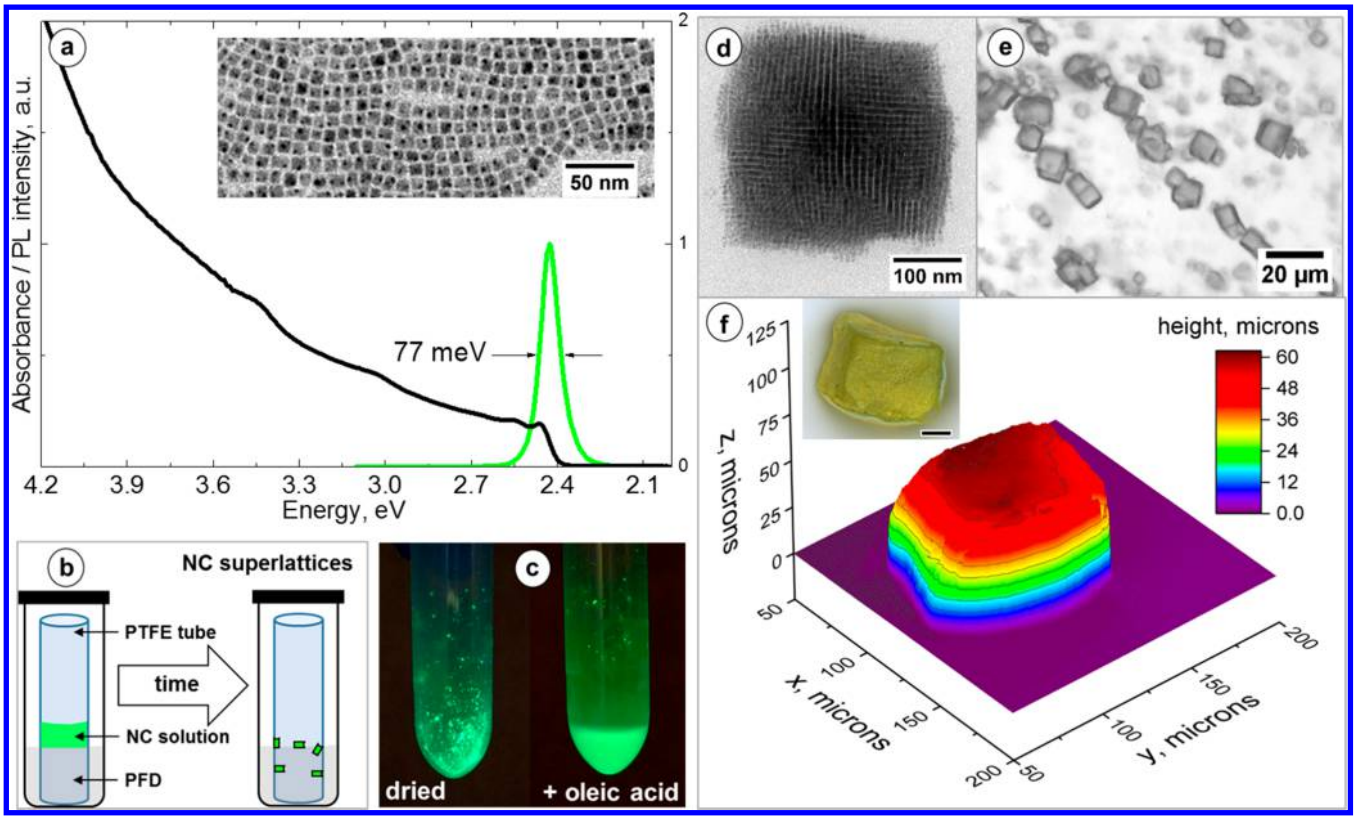

Figure 1. (a) Steady-state absorption (solid black curve) and PL (solid green curve) spectra and a low-magnification TEM image (inset) of a batch of ~6.8 ± 1 nm $CsPbBr_3$ NCs; (b) schematic of the $CsPbBr_3$ NC self-assembly on the surface of perfluorodecalin (PFD); (c) photographs of a vial with a luminescent solid of $CsPbBr_3$ NC SLs after PFD was decanted off ("dried") and after addition of oleic acid ("+oleic acid"); (d) low-magnification TEM image of a small (<1 μm) $CsPbBr_3$ NC SL showing a simple cubic packing of individual NCs. This type of packing is typical for nanocubes with sharp edges;[24] (e) optical microscopy image of the $CsPbBr_3$ NC SL suspension in oleic acid with ~10 μm SLs; (f) topology of a large SL in three dimensions and an accompanying optical image (insert, scale bar 20 μm).

octadecene (ODE, which acts as a solvent). The modifications we made to the original procedure consisted of performing the reaction in a 20 mL glass vial on a hot plate under air,[25,26] and using optimized amounts of oleic acid and oleylamine to minimize NC size distribution.[5] To decrease the amount of the remaining organics, the as-synthesized NC batches were repeatedly centrifuged in a solid form. The experimental details are provided in the Supporting Information.

Figure 1a shows the steady-state absorption and PL spectra, and a low-resolution TEM image of a representative batch of the cube-shaped $CsPbBr_3$ NCs that were used in the self-assembly experiments (see Figure S3 for size distribution). As was noted by Rainò et al.,[14] a narrow size distribution of the starting NCs is crucial for obtaining SLs. The $CsPbBr_3$ NC batches characterized by PL spectra with a full width at half maximum (fwhm) <80 meV in dilute toluene solutions (PL λ_{max} in the range 509–512 nm) were selected for self-assembly. The batches fitting that criterion were consistently observed to form layers of closely packed NCs after being drop-casted onto a TEM grid.

In our approach to making SLs, we employed liquid PFD for the interfacial self-assembly, as initial attempts to use diethylene glycol[18] resulted in the degradation of the $CsPbBr_3$ NCs (the NC solution turned dark yellow and lost its green emission). PFD, however, is a chemically inert perfluorinated liquid that is partially miscible with hexane (the reported miscibility of PFD and *n*-hexane is x_{12} = 83.59 wt % at 294.05 K,[27] which translates to ~1.73:1 PFD to hexane mixture by volume). PFD does not solubilize ligand-capped NCs so it can be used as both a substrate and an antisolvent for the NC self-assembly. The self-assembly was set up inside a well that was cut out of a PTFE tube, as is illustrated in Figure 1b (see also section S2d, Figure S4). The well creates a lipophobic and hydrophobic environment around the NC solution, thus preventing the NCs from spreading onto the surrounding surfaces while the hexane diffuses into the PFD. Depending on the amount of organic residuals that are carried with the NCs after the synthesis, the waxy solid left after the hexane diffusion could appear powdery (Figure 1c) or chunky (Figures S5 and S6). Upon inspection under an optical microscope, the solid was found to be an aggregate of NC SLs (Figures S5 and S6). A liquid suspension of NC SLs was obtained by adding a small amount of oleic acid to the solid (Figure 1c, Figures S7 and S8). The NC SLs in the suspension were inspected with the optical microscope (Figure 1e). Generally, the lateral dimensions of the obtained NC SLs were >1 μm (Figures S6–S12), and they were too thick to be viewed under TEM. However, by reducing the concentration of NCs and the volume of the NC solution that was deposited onto the surface of the PFD, it was possible to obtain smaller SLs with dimensions <1 μm and inspect them under TEM (Figure 1d). The biggest $CsPbBr_3$ NC SLs that were prepared by this method could reach up to ~70 μm (Figure 1f, Figures S6, S11, and S12). The SLs prepared by this method have isotropic shapes with similar widths, lengths, and heights (Figures S9–S12). This is in contrast to SLs that are grown by slow solvent evaporation, which were found to be flat (Figure S13). The developed self-assembly method yields SLs that can be transferred onto an

DOI: 10.1021/acs.jpclett.9b00178
J. Phys. Chem. Lett. 2019, 10, 655–660

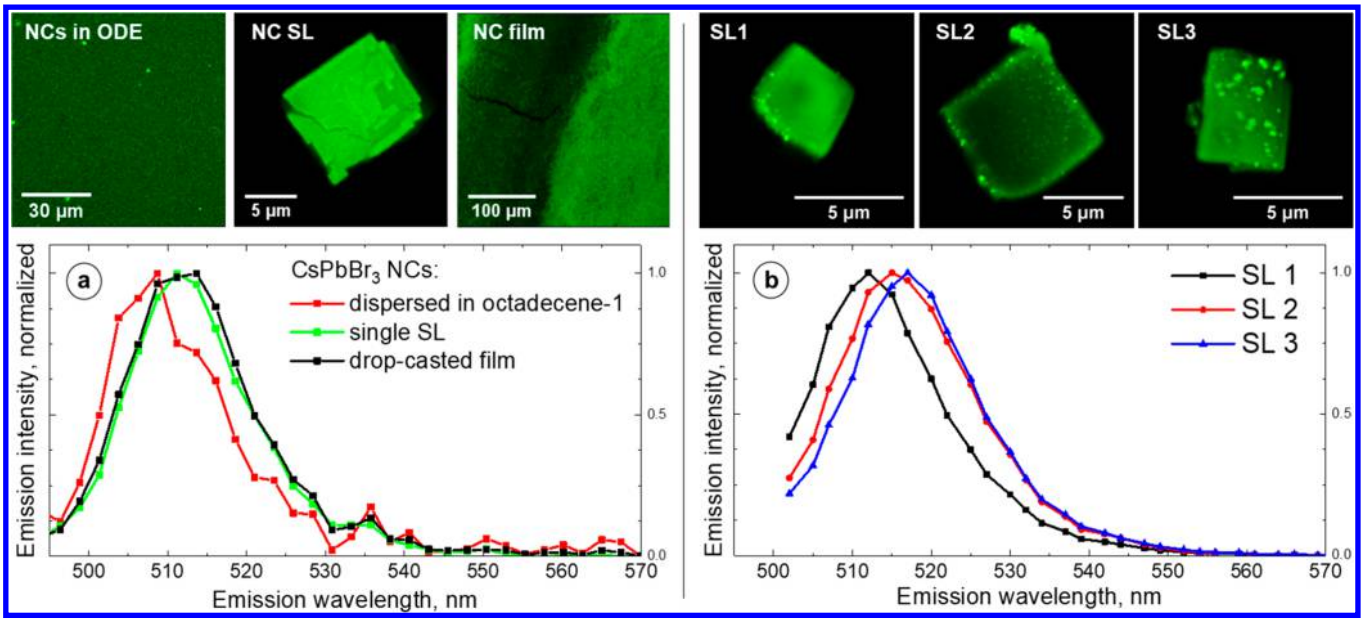

Figure 2. Confocal PL microscopy images and spectra of (a) three different $CsPbBr_3$ NC samples: NCs dispersed in ODE (red curve), an individual SL (green curve, λ_{max} = 511 nm), and a NC film drop-casted from a hexane solution (black curve). Confocal PL microscopy images and spectra of (b) Three $CsPbBr_3$ NC SLs with varying degrees of impurities and PL red shifts, SL1 (black curve, λ_{max} = 512 nm), SL2 (red curve, λ_{max} = 515 nm), SL3 (blue curve, λ_{max} = 517 nm). The samples were excited with an Ar laser, λ_{exc} = 488 nm.

arbitrary substrate with the help of ultrasonication (see section S2e and supporting video 1).

A wide range of values for a PL red shift of $CsPbBr_3$ NC SLs have been reported, as noted above.[3,7,15,20−23] These conflicting findings motivated us to explore the possible causes of the large PL red shift. First, the PL of individual SLs was investigated. Three samples that derived from the same batch of $CsPbBr_3$ NCs were examined by confocal PL microscopy: an oleic acid dispersion of SLs, a film drop-casted from the hexane solution of NCs;, and a NC solution in ODE. ODE was chosen as a solvent for the NCs due to its high boiling point (toluene and hexane are too volatile for this experiment). Figure 2a shows the comparison between the spectra (see Figure S14 for additional spectra).

The PL spectra of both isolated NC SLs and a drop-casted NC film are similar, peaking at ∼511−512 nm (2.426−2.422 eV) with ∼84−85 meV fwhm. These spectra are red-shifted and broadened in comparison to the PL spectrum of a NC solution in ODE, which peaks at ∼509 nm (2.436 eV) and has a PL fwhm of ∼79 meV. Another experiment that was performed on a different batch of $CsPbBr_3$ NCs showed qualitatively similar results—a small red shift in the PL peak and a broadening of the spectrum in the film or SL (Figures S15 and S16). A ∼ 2−3 nm (∼10−15 meV) PL red shift was observed for individual SLs, which is significantly smaller than the ∼96 meV red shift that was observed in the aggregates of SLs (Figure S1). This modest red shift is consistent with our prior report[7] and is within the range 0−30 meV, which was reported by van der Burgt et al.[20]

Interestingly, in addition to SLs with a spatially uniform PL across their surface (Figure 2a), we observed SLs covered with bright spots. We noticed that there is a correlation between the number of bright spots and the extent of the PL red shift: the more spots the SLs have, the larger the PL red shift is (Figure 2b, up to ∼40 meV for SL3 in comparison to NCs in dilute solution). A series of spectrally resolved slices were recorded as a function of the thickness (z slices) for clean SLs and the SLs with spots. The resulting series indicated that the spots are located on the surfaces of SLs (Figures S17−S25). The SLs with spots on the surface were examined by high resolution scanning electron microscopy (HRSEM). The spots appear as bright objects of rhombic and rectangular shapes with sharp edges, ∼50−300 nm in size (Figures S26−S28). The energy dispersive X-ray spectroscopy (EDS) mapping did not reveal significant deviations from $CsPbBr_3$ stoichiometry (Figure S28, Table S1). We interpret these objects as submicrometer crystals of $CsPbBr_3$ formed because of NC degradation or coalescence. Such submicrometer crystals have a red-shifted PL compared to the NCs due to the loss of quantum confinement [optical bandgap of bulk $CsPbBr_3$ is ∼2.25 eV (∼550 nm).[28] The presence of luminescent impurities on top of the LHP NC SLs has not been reported previously. Interestingly, it bears similarity to the surfaces of LHP single crystals; the differences in the structure[29] and composition[30] of the surfaces have been proposed as one of the explanations for a dual PL observed in bulk samples.

A PL red shift in $CsPbBr_3$ NC SLs can also occur as a result of a photon propagation effect,[23] by which we mean a combination of PL self-absorption and a concomitant re-emission by the NCs with a matching bandgap. The photon propagation effect has been reported to red shift the PL in bulk LHP (by ∼130 meV in crystals of $CH_3NH_3PbBr_3$[31] and by ∼70 meV in thin films of $CH_3NH_3PbI_3$[32]), but it has not been studied in NC SLs. In the case of self-absorption alone, an experimentally measured PL is affected by the transmission of the NCs' PL through the surrounding NCs, because the PL Stokes shift is small (Figure 1a). It is anticipated that the magnitude of the PL red shift due to the self-absorption depends on the amount of the material in the sample.

To explore how a PL red shift responds to the relative amount of SLs, we recorded PL spectra from three macroscopic areas on the 2 in. diameter Si wafer that was covered with a variable density of $CsPbBr_3$ NC SLs. For this experiment, a batch of shape-pure cubic $CsPbBr_3$ NCs with an edge length of 8.5 ± 0.5 nm was used. Briefly, a batch of $CsPbBr_3$ NCs with a PL λ_{max} =

DOI: 10.1021/acs.jpclett.9b00178
J. Phys. Chem. Lett. 2019, 10, 655−660

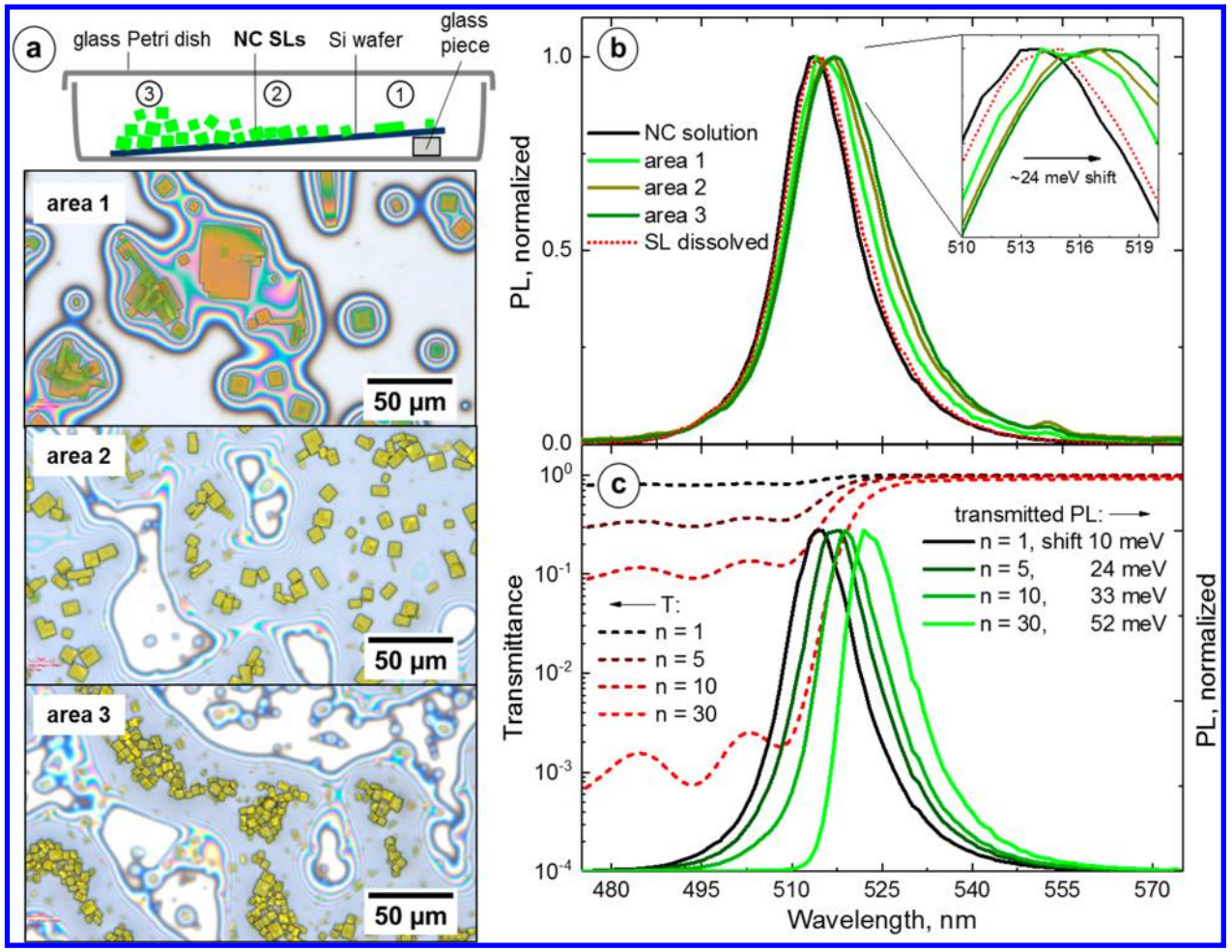

Figure 3. (a) Scheme of the $CsPbBr_3$ NC SLs that were grown on a tilted Si wafer by a slow solvent evaporation and optical microscopy images of three areas on the wafer with different densities of NC SLs. (b) PL spectra from the areas with a different SL coverage (a small peak near 555 nm is possibly an artifact). (c) Effect of the self-absorption on the measured PL. Short-dashed lines are transmission spectra at four different extinctions, and solid lines are the resulting PL spectra.

512 nm (fwhm = 70 meV) was synthesized using the benzoyl bromide route[33] involving oleic acid and didodecylamine ligands.[7,33] The self-assembly was performed by slow solvent evaporation from a toluene solution of NCs on a tilted Si wafer (Figure 3a), as described in our recent work.[7] Performing the self-assembly on a tilted Si wafer yielded a spatial gradient of the SL coverage (Figure 3a): from an area with thin, well-isolated SLs (area 1) to an area with thicker, closely packed SLs (area 2), then to an area where SLs were bunched on top of each other (area 3). The PL spectra for these areas are shown in Figure 3b. The PL spectra of individual SLs with a clean surface are broadened and red-shifted slightly compared to the spectra of NCs in solution (Figure S29), and this is consistent with the results discussed above (Figure 2a). An examination of the sample with a confocal PL setup did not reveal any SLs with impurities (Figure S29), so we can rule out their influence on the PL red shift in this experiment. Both the PL red shift (from 512 to 517 nm, ~24 meV) and the spectral broadening (from 70 to 87 meV, respectively) increased gradually from NCs in solution to SL aggregates (Figure 3b).

To determine whether or not the PL red shift is due to the self-absorption alone, we treated the sample as an absorbing filter with a transmission spectrum of a dilute toluene solution of $CsPbBr_3$ NCs: $T(n,\lambda) = 10^{-n\cdot A(\lambda)}$, where T is transmittance, n is a multiplicative constant, and A is absorbance. The multiplicative constant is introduced to simulate different volumes of the material. In other words, increasing n is akin to increasing the thickness of the sample, which leads to a decrease in the transmittance. Next, we obtained a series of self-transmitted PL spectra as a function of n (Figure 3c, dashed curves): $I_{PL}^{ST}(n,\lambda) = I_{PL}(\lambda)\cdot T(n,\lambda)$, where $I_{PL}(\lambda)$ is a PL spectrum of the same dilute toluene solution of $CsPbBr_3$ NCs. Upon comparison of $I_{PL}^{ST}(n,\lambda)$ for different n values (n = 1, 5, 10, 30), the PL λ_{max} shifts from 514 to 523 nm (Figure 3c, solid curves). This shift is accompanied by a change in the shape of the PL spectrum (especially noticeable at n = 30): the spectrum narrows and becomes steeper on the high energy side (thus, self-absorption may explain prior observations of asymmetric PL spectra of $CsPbBr_3$ NC SLs[15]).

To summarize, a PL red shift in $CsPbBr_3$ NC SLs with magnitudes from ~10−15 meV (isolated SLs with clean surfaces) to ~96 meV (aggregates of SLs) has been observed for various samples studied in this work. The ~10−15 meV PL red shift in isolated SLs is interpreted as a combination of three effects: changes in the dielectric environment, electronic coupling between the NCs, and the photon propagation. The large ~96 meV PL red shift measured for the aggregates of SLs arises from two additional factors: the presence of SLs with

DOI: 10.1021/acs.jpclett.9b00178
J. Phys. Chem. Lett. 2019, 10, 655−660

impurities of bulklike $CsPbBr_3$ particles on their surface, which adds ~30 meV or more to the PL red shift, and the photon propagation effect, the magnitude of which depends on the volume of the material in the sample (self-absorption is enough to contribute >50 meV of additional PL red shift in a macroscopic sample). The PL red shift in all of the SL samples studied in this work is accompanied by the broadening of PL spectra, which is the opposite of the narrowing that is expected in the case of self-absorption alone (Figure 3c and experimental observations reported in refs 31, 32, 34, and 35). Two possible causes of the PL broadening are the increased contribution into PL from the NCs with smaller bandgaps (bigger sizes) due to the interparticle energy transfer[36−38] and the energetic disorder due to localized variations in the dielectric environment caused by the defects inside SLs.[20]

■ ASSOCIATED CONTENT

Supporting Information

The Supporting Information is available free of charge on the ACS Publications website at DOI: 10.1021/acs.jpclett.9b00178.

PL spectra of SLs samples, experimental details, size determination of $CsPbBr_3$ NCs by TEM, photographs of the self-assembly setup, optical microscopy images of NC SLs in solid and dispersion, optical profilometry of $CsPbBr_3$ NC SLs, HRSEM analysis of impurities on the surface of SLs, confocal PL microscopy images and z slices of $CsPbBr_3$ NC SLs (PDF)

Video displaying transfer of $CsPbBr_3$ NC SLs onto silicon wafer under ultrasonication (AVI)

■ AUTHOR INFORMATION

Corresponding Authors

*E-mail: dmitry.baranov@iit.it.
*E-mail: liberato.manna@iit.it.

ORCID

Dmitry Baranov: 0000-0001-6439-8132
Muhammad Imran: 0000-0001-7091-6514
Liberato Manna: 0000-0003-4386-7985

Notes

The authors declare no competing financial interest.

■ ACKNOWLEDGMENTS

The work of D.B. was supported by the European Union's Horizon 2020 research and innovation programme under the Marie Sklodowska-Curie grant agreement No. 794560 (RETAIN). The work of S.T., M.I., and L.M. was supported by the European Union under grant agreement No. 614897 (ERC Grant TRANS-NANO). We thank Quinten Akkerman and Dr. Guilherme Almeida for advice on the synthesis of $CsPbBr_3$ NCs, Simone Lauciello (Electron Microscopy Facility at IIT) for help with HRSEM/EDS analysis of SLs, and Michele Oneto (Nikon Center at IIT) for assistance with confocal PL microscopy on SLs grown by a slow solvent evaporation.

■ REFERENCES

(1) Protesescu, L.; Yakunin, S.; Bodnarchuk, M. I.; Krieg, F.; Caputo, R.; Hendon, C. H.; Yang, R. X.; Walsh, A.; Kovalenko, M. V. Nanocrystals of Cesium Lead Halide Perovskites ($CsPbX_3$, X = Cl, Br, and I): Novel Optoelectronic Materials Showing Bright Emission with Wide Color Gamut. *Nano Lett.* **2015**, *15*, 3692−3696.

(2) Akkerman, Q. A.; Rainò, G.; Kovalenko, M. V.; Manna, L. Genesis, challenges and opportunities for colloidal lead halide perovskite nanocrystals. *Nat. Mater.* **2018**, *17*, 394−405.

(3) Kovalenko, M. V.; Protesescu, L.; Bodnarchuk, M. I. Properties and potential optoelectronic applications of lead halide perovskite nanocrystals. *Science* **2017**, *358*, 745−750.

(4) Akkerman, Q. A.; D'Innocenzo, V.; Accornero, S.; Scarpellini, A.; Petrozza, A.; Prato, M.; Manna, L. Tuning the Optical Properties of Cesium Lead Halide Perovskite Nanocrystals by Anion Exchange Reactions. *J. Am. Chem. Soc.* **2015**, *137*, 10276−10281.

(5) Almeida, G.; Goldoni, L.; Akkerman, Q.; Dang, Z.; Khan, A. H.; Marras, S.; Moreels, I.; Manna, L. Role of Acid−Base Equilibria in the Size, Shape, and Phase Control of Cesium Lead Bromide Nanocrystals. *ACS Nano* **2018**, *12*, 1704−1711.

(6) Dong, Y.; Qiao, T.; Kim, D.; Parobek, D.; Rossi, D.; Son, D. H. Precise Control of Quantum Confinement in Cesium Lead Halide Perovskite Quantum Dots via Thermodynamic Equilibrium. *Nano Lett.* **2018**, *18*, 3716−3722.

(7) Imran, M.; Ijaz, P.; Baranov, D.; Goldoni, L.; Petralanda, U.; Akkerman, Q.; Abdelhady, A. L.; Prato, M.; Bianchini, P.; Infante, I.; et al. Shape-Pure, Nearly Monodispersed $CsPbBr_3$ Nanocubes Prepared Using Secondary Aliphatic Amines. *Nano Lett.* **2018**, *18*, 7822−7831.

(8) Boles, M. A.; Engel, M.; Talapin, D. V. Self-Assembly of Colloidal Nanocrystals: From Intricate Structures to Functional Materials. *Chem. Rev.* **2016**, *116*, 11220−11289.

(9) Murray, C. B.; Kagan, C. R.; Bawendi, M. G. Synthesis and Characterization of Monodisperse Nanocrystals and Close-Packed Nanocrystal Assemblies. *Annu. Rev. Mater. Sci.* **2000**, *30*, 545−610.

(10) Collier, C. P.; Vossmeyer, T.; Heath, J. R. Nanocrystal Superlattices. *Annu. Rev. Phys. Chem.* **1998**, *49*, 371−404.

(11) Abécassis, B. Three-Dimensional Self Assembly of Semiconducting Colloidal Nanocrystals: From Fundamental Forces to Collective Optical Properties. *ChemPhysChem* **2016**, *17*, 618−631.

(12) Vanmaekelbergh, D. Self-assembly of colloidal nanocrystals as route to novel classes of nanostructured materials. *Nano Today* **2011**, *6*, 419−437.

(13) Jurow, M. J.; Lampe, T.; Penzo, E.; Kang, J.; Koc, M. A.; Zechel, T.; Nett, Z.; Brady, M.; Wang, L.-W.; Alivisatos, A. P.; et al. Tunable Anisotropic Photon Emission from Self-Organized $CsPbBr_3$ Perovskite Nanocrystals. *Nano Lett.* **2017**, *17*, 4534−4540.

(14) Rainò, G.; Becker, M. A.; Bodnarchuk, M. I.; Mahrt, R. F.; Kovalenko, M. V.; Stöferle, T. Superfluorescence from Lead Halide Perovskite Quantum Dot Superlattices. *Nature* **2018**, *563*, 671−675.

(15) Tong, Y.; Yao, E.-P.; Manzi, A.; Bladt, E.; Wang, K.; Döblinger, M.; Bals, S.; Müller-Buschbaum, P.; Urban, A. S.; Polavarapu, L.; et al. Spontaneous Self-Assembly of Perovskite Nanocrystals into Electronically Coupled Supercrystals: Toward Filling the Green Gap. *Adv. Mater.* **2018**, *30*, 1801117.

(16) Kim, Y.; Yassitepe, E.; Voznyy, O.; Comin, R.; Walters, G.; Gong, X.; Kanjanaboos, P.; Nogueira, A. F.; Sargent, E. H. Efficient Luminescence from Perovskite Quantum Dot Solids. *ACS Appl. Mater. Interfaces* **2015**, *7*, 25007−25013.

(17) Talapin, D. V.; Shevchenko, E. V.; Kornowski, A.; Gaponik, N.; Haase, M.; Rogach, A. L.; Weller, H. A New Approach to Crystallization of CdSe Nanoparticles into Ordered Three-Dimensional Superlattices. *Adv. Mater.* **2001**, *13*, 1868−1871.

(18) Dong, A.; Chen, J.; Vora, P. M.; Kikkawa, J. M.; Murray, C. B. Binary nanocrystal superlattice membranes self-assembled at the liquid−air interface. *Nature* **2010**, *466*, 474−477.

(19) Murray, C. B.; Kagan, C. R.; Bawendi, M. G. Self-Organization of CdSe Nanocrystallites into Three-Dimensional Quantum Dot Superlattices. *Science* **1995**, *270*, 1335−1338.

(20) van der Burgt, J. S.; Geuchies, J. J.; van der Meer, B.; Vanrompay, H.; Zanaga, D.; Zhang, Y.; Albrecht, W.; Petukhov, A. V.; Filion, L.; Bals, S.; et al. Cuboidal Supraparticles Self-Assembled from Cubic $CsPbBr_3$ Perovskite Nanocrystals. *J. Phys. Chem. C* **2018**, *122*, 15706−15712.

DOI: 10.1021/acs.jpclett.9b00178
J. Phys. Chem. Lett. 2019, 10, 655−660

(21) Wang, K.-H.; Yang, J.-N.; Ni, Q.-K.; Yao, H.-B.; Yu, S.-H. Metal Halide Perovskite Supercrystals: Gold−Bromide Complex Triggered Assembly of $CsPbBr_3$ Nanocubes. *Langmuir* **2018**, *34*, 595−602.
(22) Kovalenko, M. V.; Bodnarchuk, M. I. Lead Halide Perovskite Nanocrystals: From Discovery to Self-assembly and Applications. *Chimia* **2017**, *71*, 461−470.
(23) Nagaoka, Y.; Hills-Kimball, K.; Tan, R.; Li, R.; Wang, Z.; Chen, O. Nanocube Superlattices of Cesium Lead Bromide Perovskites and Pressure-Induced Phase Transformations at Atomic and Mesoscale Levels. *Adv. Mater.* **2017**, *29*, 1606666.
(24) Wang, D.; Hermes, M.; Kotni, R.; Wu, Y.; Tasios, N.; Liu, Y.; de Nijs, B.; van der Wee, E. B.; Murray, C. B.; Dijkstra, M.; et al. Interplay between spherical confinement and particle shape on the self-assembly of rounded cubes. *Nat. Commun.* **2018**, *9*, 2228.
(25) Akkerman, Q.; Martínez-Sarti, L.; Goldoni, L.; Imran, M.; Baranov, D.; Bolink, H. J.; Palazon, F.; Manna, L. Molecular Iodine for a General Synthesis of Binary and Ternary Inorganic and Hybrid Organic−Inorganic Iodide Nanocrystals. *Chem. Mater.* **2018**, *30*, 6915−6921.
(26) Akkerman, Q. A.; Park, S.; Radicchi, E.; Nunzi, F.; Mosconi, E.; De Angelis, F.; Brescia, R.; Rastogi, P.; Prato, M.; Manna, L. Nearly Monodisperse Insulator Cs_4PbX_6 (X = Cl, Br, I) Nanocrystals, Their Mixed Halide Compositions, and Their Transformation into $CsPbX_3$ Nanocrystals. *Nano Lett.* **2017**, *17*, 1924−1930.
(27) Bernardo-Gil, G. S.; Soares, L. J. S. Mutual binary solubilities: Perfluorodecalin/hydrocarbons. *J. Chem. Eng. Data* **1987**, *32*, 327−329.
(28) Stoumpos, C. C.; Malliakas, C. D.; Peters, J. A.; Liu, Z.; Sebastian, M.; Im, J.; Chasapis, T. C.; Wibowo, A. C.; Chung, D. Y.; Freeman, A. J.; et al. Crystal Growth of the Perovskite Semiconductor $CsPbBr_3$: A New Material for High-Energy Radiation Detection. *Cryst. Growth Des.* **2013**, *13*, 2722−2727.
(29) Sheikh, T.; Shinde, A.; Mahamuni, S.; Nag, A. Possible Dual Bandgap in $(C_4H_9NH_3)_2PbI_4$ 2D Layered Perovskite: Single-Crystal and Exfoliated Few-Layer. *ACS Energy Lett.* **2018**, *3*, 2940−2946.
(30) Chi, X.; Leng, K.; Wu, B.; Shi, D.; Choy, Y.; Chen, Z.; Chen, Z.; Yu, X.; Yang, P.; Xu, Q.-H.; et al. Elucidating Surface and Bulk Emission in 3D Hybrid Organic−Inorganic Lead Bromide Perovskites. *Adv. Opt. Mater.* **2018**, *6*, 1800470.
(31) Fang, Y.; Wei, H.; Dong, Q.; Huang, J. Quantification of re-absorption and re-emission processes to determine photon recycling efficiency in perovskite single crystals. *Nat. Commun.* **2017**, *8*, 14417.
(32) Pazos-Outón, L. M.; Szumilo, M.; Lamboll, R.; Richter, J. M.; Crespo-Quesada, M.; Abdi-Jalebi, M.; Beeson, H. J.; Vrućinić, M.; Alsari, M.; Snaith, H. J.; et al. Photon recycling in lead iodide perovskite solar cells. *Science* **2016**, *351*, 1430−1433.
(33) Imran, M.; Caligiuri, V.; Wang, M.; Goldoni, L.; Prato, M.; Krahne, R.; De Trizio, L.; Manna, L. Benzoyl Halides as Alternative Precursors for the Colloidal Synthesis of Lead-Based Halide Perovskite Nanocrystals. *J. Am. Chem. Soc.* **2018**, *140*, 2656−2664.
(34) Di Stasio, F.; Imran, M.; Akkerman, Q. A.; Prato, M.; Manna, L.; Krahne, R. Reversible Concentration-Dependent Photoluminescence Quenching and Change of Emission Color in $CsPbBr_3$ Nanowires and Nanoplatelets. *J. Phys. Chem. Lett.* **2017**, *8*, 2725−2729.
(35) Koc, M. A.; Raja, S. N.; Hanson, L. A.; Nguyen, S. C.; Borys, N. J.; Powers, A. S.; Wu, S.; Takano, K.; Swabeck, J. K.; Olshansky, J. H.; et al. Characterizing Photon Reabsorption in Quantum Dot-Polymer Composites for Use as Displacement Sensors. *ACS Nano* **2017**, *11*, 2075−2084.
(36) Zhitomirsky, D.; Kramer, I. J.; Labelle, A. J.; Fischer, A.; Debnath, R.; Pan, J.; Bakr, O. M.; Sargent, E. H. Colloidal Quantum Dot Photovoltaics: The Effect of Polydispersity. *Nano Lett.* **2012**, *12*, 1007−1012.
(37) Kagan, C. R.; Murray, C. B. Charge transport in strongly coupled quantum dot solids. *Nat. Nanotechnol.* **2015**, *10*, 1013−1026.
(38) Akselrod, G. M.; Prins, F.; Poulikakos, L. V.; Lee, E. M. Y.; Weidman, M. C.; Mork, A. J.; Willard, A. P.; Bulović, V.; Tisdale, W. A. Subdiffusive Exciton Transport in Quantum Dot Solids. *Nano Lett.* **2014**, *14*, 3556−3562.

DOI: 10.1021/acs.jpclett.9b00178
J. Phys. Chem. Lett. 2019, 10, 655−660